

Dielectronic recombination of heavy species: the tin
 $4p^6 4d^q - 4p^6 4d^{(q-1)} 4f + 4p^5 4d^{(q+1)}$ transition arrays for
 $q = 1 - 9$

Nigel Badnell

Department of Physics
University of Strathclyde
Glasgow, UK

Collaborators

Adam Foster (ex Culham, now Harvard-Smithsonian Center for Astrophysics)

Don Griffin (Rollins College)

Deirdre Kilbane (University College Dublin)

Martin O Mullane and Hugh Summers (Strathclyde/JET)

Introduction

- Dielectronic recombination establishes plasma ionization balance in competition with ionization — necessary for astrophysical, magnetic fusion and technical plasmas.
- Heavy species for ITER and ITER-like devices are computationally demanding compared to the light elements previously needed by JET and much of astrophysics.
- Report on recently completed major study of the Tin open 4d-subshell.
- Highly relevant to Tungsten: W^{35+} is isoelectronic with Sn^{11+} — compare and contrast with Ballance et al.
- Tin of interest to EUV (13.5 nm) microlithography.
- Tin probe used on Mega Amp Spherical Tokamak (MAST) to study marker species diagnostics and impurity transport.

Theory

The partial dielectronic recombination rate coefficient α_{fi}^z from an initial state i of an ion X^{+z} into a resolved final state f of an ion X^{+z-1} is given by

$$\alpha_{fi}^z(T) = \left(\frac{4\pi a_0^2 I_H}{k_B T_e} \right)^{3/2} \sum_j \frac{\omega_j}{2\omega_i} e^{-E_c/(k_B T_e)} \times \frac{\sum_l A_{j \rightarrow i, E_{cl}}^a A_{j \rightarrow f}^r}{\sum_h A_{j \rightarrow h}^r + \sum_{m,l} A_{j \rightarrow m, E_{cl}}^a} \quad (1)$$

in the isolated resonance approximation. Here ω_j is the statistical weight of the $(N + 1)$ -electron doubly-excited resonance state j , ω_i is the statistical weight of the N -electron target state (so, $z = Z - N$) and the autoionization (A^a) and radiative (A^r) rates are in inverse seconds. E_c is the energy of the continuum electron (with orbital angular momentum l) which is fixed by the position of the resonances and I_H is the ionization potential energy of the hydrogen atom (both in the same units of energy), k_B is the Boltzman constant, T_e the electron temperature and $(4\pi a_0^2)^{3/2} = 6.6011 \times 10^{-24} \text{ cm}^3$.

Implementation

- AUTOSTRUCTURE

Pros: level-resolved, Breit-Pauli, kappa-averaged Dirac equation, N - and $(N + 1)$ -electron CI.

Cons: CPU demanding (esp. memory).

- Burgess-Bethe (General Program)

Pros: j-resolved core/target core uncoupled from bundled- n lRydberg/continuum, N -electron CI, fast.

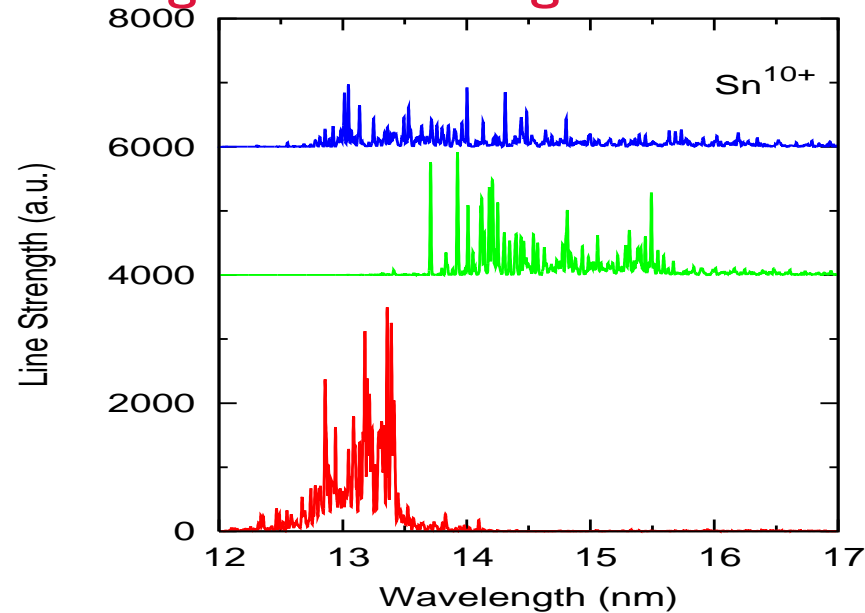
Cons: dipole autoionization only, no $(N + 1)$ -electron CI.

- Configuration-Average

Pros: includes non-dipole autoionization, fast.

Cons: no CI, config is either bound or autoionizing, no level-resolution.

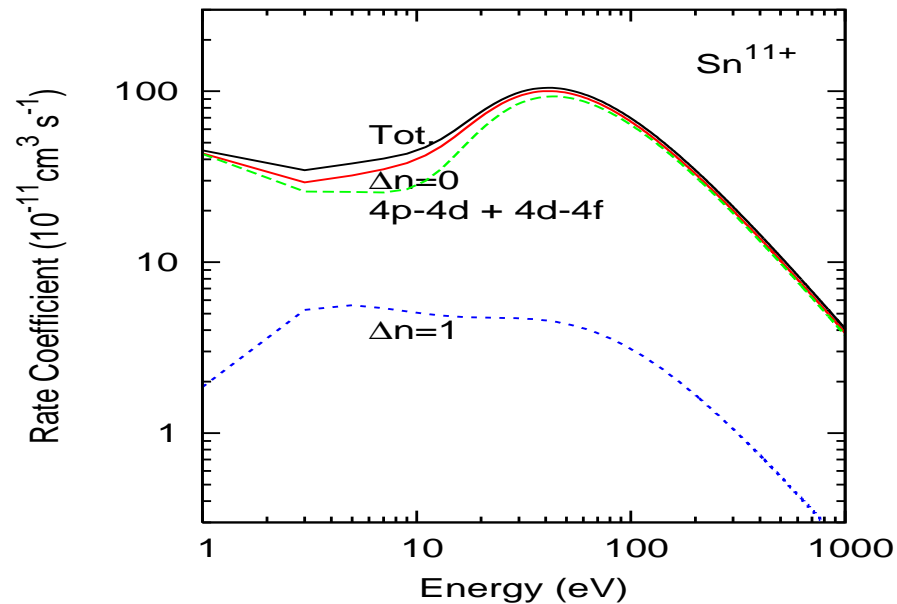
Configuration-mixing



Total line strength emission in Sn^{10+} as function of wavelength convoluted with a 0.01 nm FWHM Gaussian. The top spectrum is from the $4p - 4d$ array and the middle from the $4d - 4f$ array and where each has been calculated separately. The bottom spectrum is the configuration-mixed ($4p^6 4d^3 4f$ with $4p^5 4d^5$) sum of $4p - 4d$ plus $4d - 4f$. See text for details. All this work.

- If all autoionizing levels satisfy either $A^r \ll A^a$ or $A^r \gg A^a$ then to a first approximation the *total* dielectronic recombination rate coefficient is unchanged by the unitary configuration-mixing transformation.

Sn¹¹⁺: DR contributions

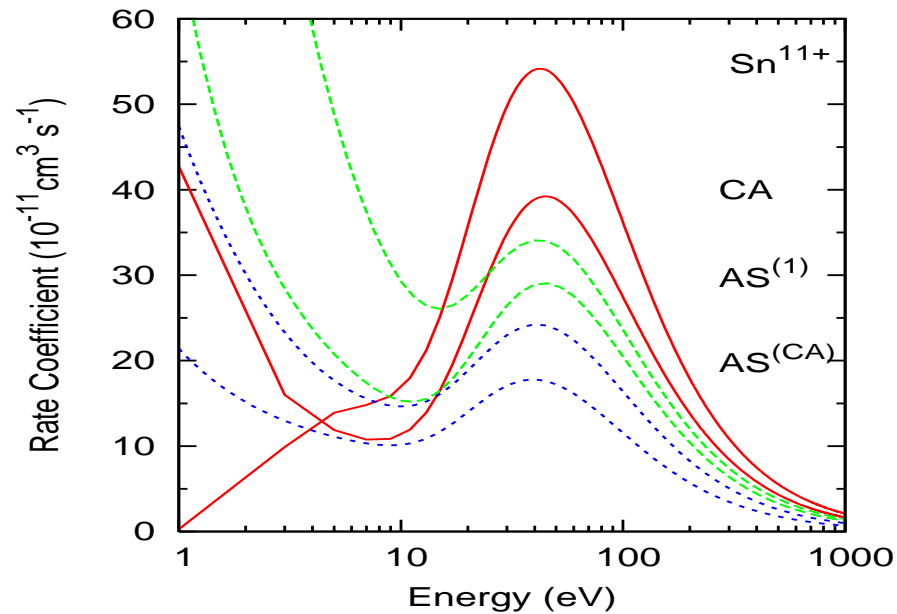


Configuration-average dielectronic recombination contributions for Sn¹¹⁺. $\Delta n = 0$ denotes the sum of the $4l - 4l'$ contributions and $\Delta n = 1$ the sum of the $4l - 5l'$. Tot. denotes the sum of the $\Delta n = 0$ plus $\Delta n = 1$. See text for details. All this work.

- Dipole $\Delta n = 0$ largely dominate — this is in contrast to W³⁵⁺. Higher-charge means excited core levels can support more N+1 bound states.

Initial Levels

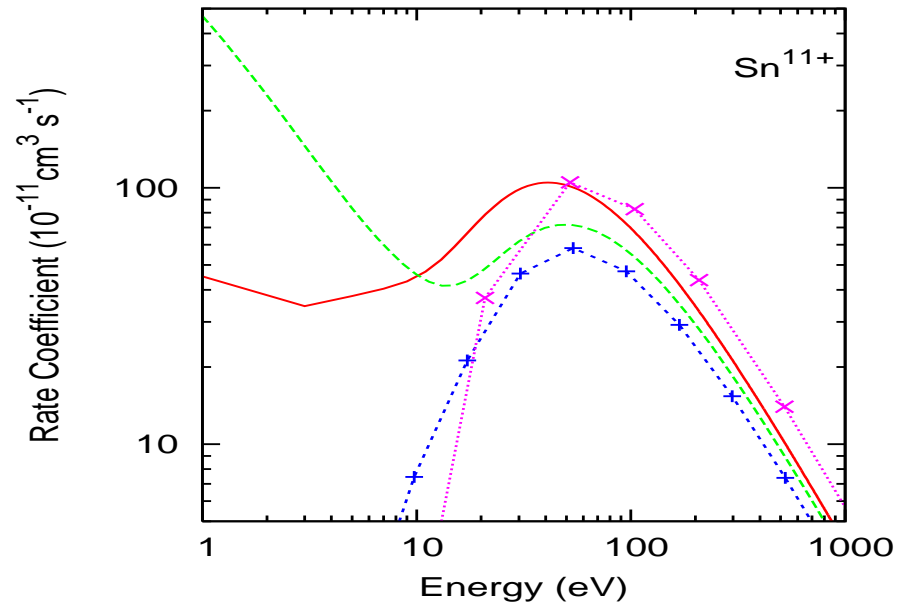
- CA averages over statistical weight of initial ground configuration.
- AS and BBGP are free to average over any user-specified initial levels.
- Generalized Collisional-Radiative modelling resolves all initial levels with significant populations (and which are not in quasi-static equilibrium with the ground level).
- So, the question is not really which initial levels to average over since they should be kept resolved for CR modelling.
- But rather, which is meaningful for comparison with CA? And, correspondingly, how should one best use CA data in a metastable/level -resolved picture?



Dielectronic recombination $4p - 4d$ and $4d - 4f$ contributions for Sn^{11+} . Solid (red) curves: configuration-average (CA); long-dashed (green) curves: AUTOSTRUCTURE averaged over the initial ground level only; short-dashed (blue) curves: AUTOSTRUCTURE averaged over all levels of the ground configuration. For each pair of curves the upper corresponds to the $4p - 4d$ contribution and the lower one the $4d - 4f$ contribution. See text for details. All this work.

- DR from excited *levels* is suppressed by alternate Auger channels.
- DR from excited *configurations* is suppressed by alternate Auger channels.

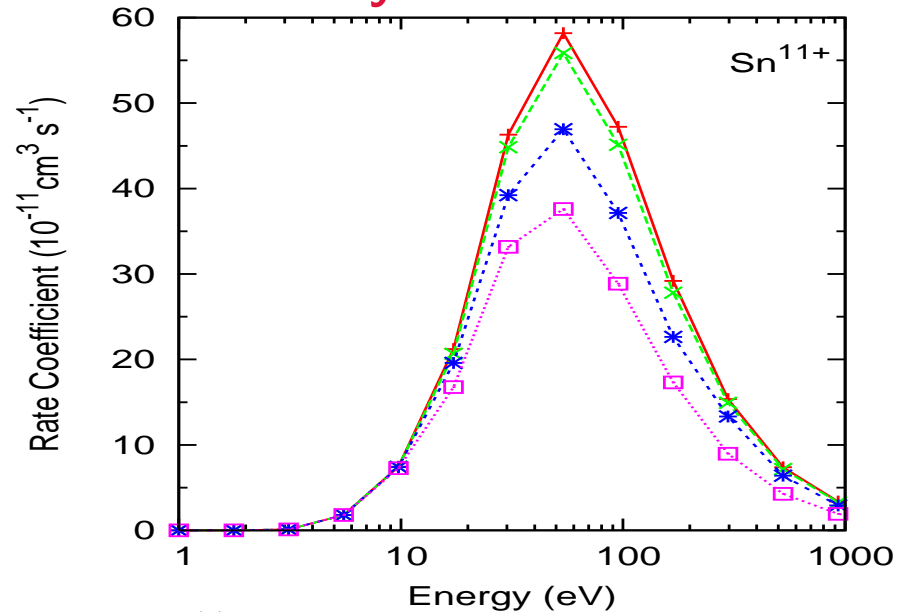
Sn¹¹⁺: Total DR



Total dielectronic recombination rate coefficients for Sn¹¹⁺. Solid (red) curve: configuration-average; long-dashed (green) curve: AUTOSTRUCTURE averaged over the initial ground level; short-dashed (blue) curve: Burgess–Bethe General Program averaged over the initial ground level; dotted (purple) curve; Burgess General Formula. All this work.

- CA results are about 45% larger and the BBGP 20% smaller than the AUTOSTRUCTURE results at the high temperature peak.
- AS configuration-mixing results are only 10% larger than the unmixed.

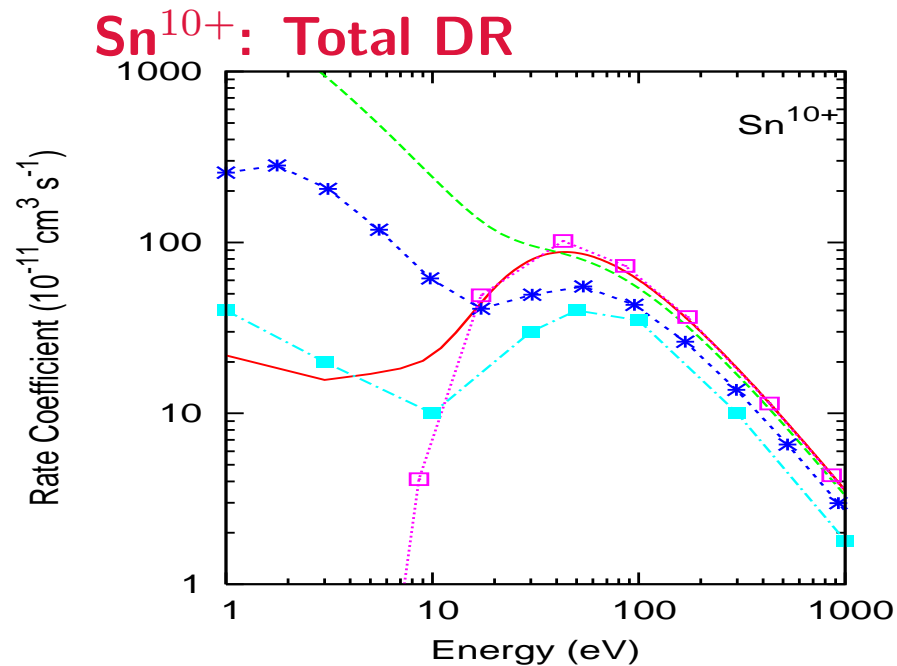
Sn¹¹⁺: Density Effects



Total dielectronic recombination rate coefficients for Sn¹¹⁺ as a function of electron density. Solid (red) curve: 10^{10} cm³/s; long-dashed (green) curve: 4.6×10^{11} cm³/s; short-dashed (blue) curve: 2.2×10^{13} cm³/s; dotted (purple) curve; 10^{15} cm³/s.

See text for details. All this work.

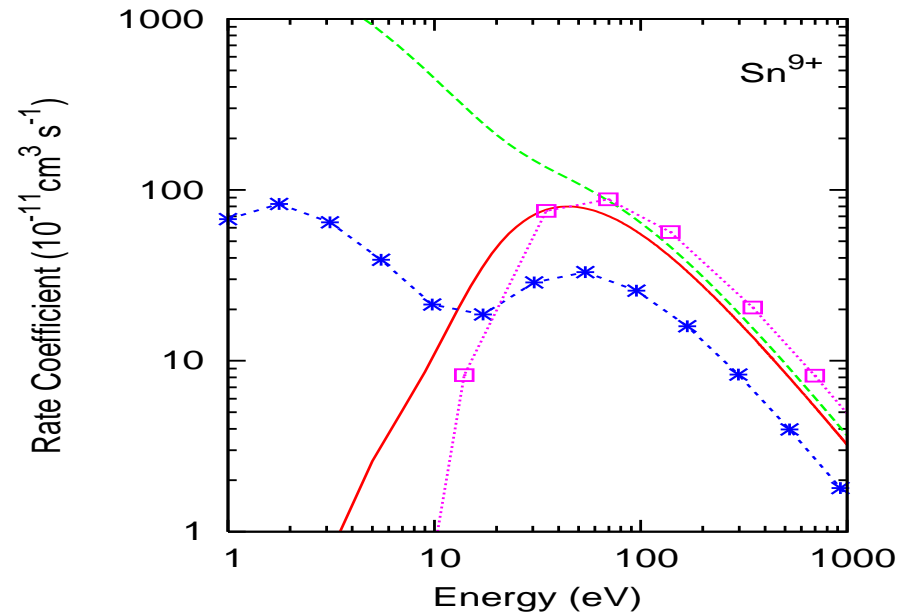
- Determined using the ADAS *baseline* approach i.e. the BBGP for dielectronic recombination.
- Negligible below $\sim 10^{11}$ cm³/s. Reduces the peak rate coefficient by 20% at $\sim 10^{13}$ cm³/s and by a nearly a factor of two at $\sim 10^{15}$ cm³/s.



Total dielectronic recombination rate coefficients for Sn¹⁰⁺. Solid (red) curve: configuration-average; long-dashed (green) curve: AUTOSTRUCTURE averaged over the initial ground level; short-dashed (blue) curve: Burgess–Bethe General Program averaged over the initial ground level; dotted (purple) curve; Burgess General Formula: all this work. Dot-dashed (cyan) curve, FAC results.

- CA results are about 50% larger, the BBGP 15% smaller and FAC 30% smaller than the AUTOSTRUCTURE results at the high temperature peak (on subtracting the different ‘low- T ’ contributions to the high- T peak.)

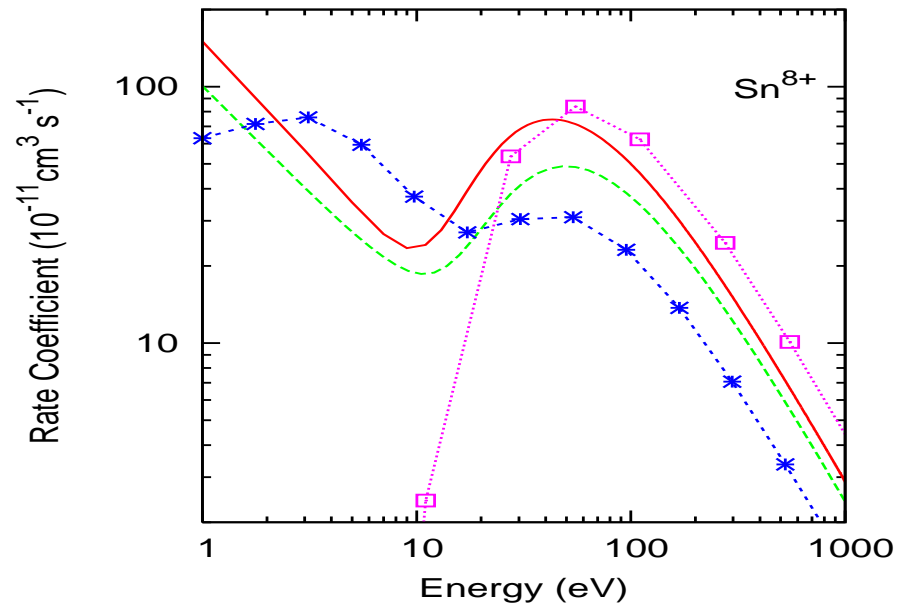
Sn⁹⁺: Total DR



Total dielectronic recombination rate coefficients for Sn⁹⁺. Solid (red) curve: configuration-average; long-dashed (green) curve: AUTOSTRUCTURE averaged over the initial ground level; short-dashed (blue) curve: Burgess-Bethe General Program averaged over the initial ground level; dotted (purple) curve: Burgess General Formula. All this work.

- CA results are about 45% larger and the BBGP 45% smaller than the AUTOSTRUCTURE results at the high temperature peak (again compensating for the low- T contribution.)

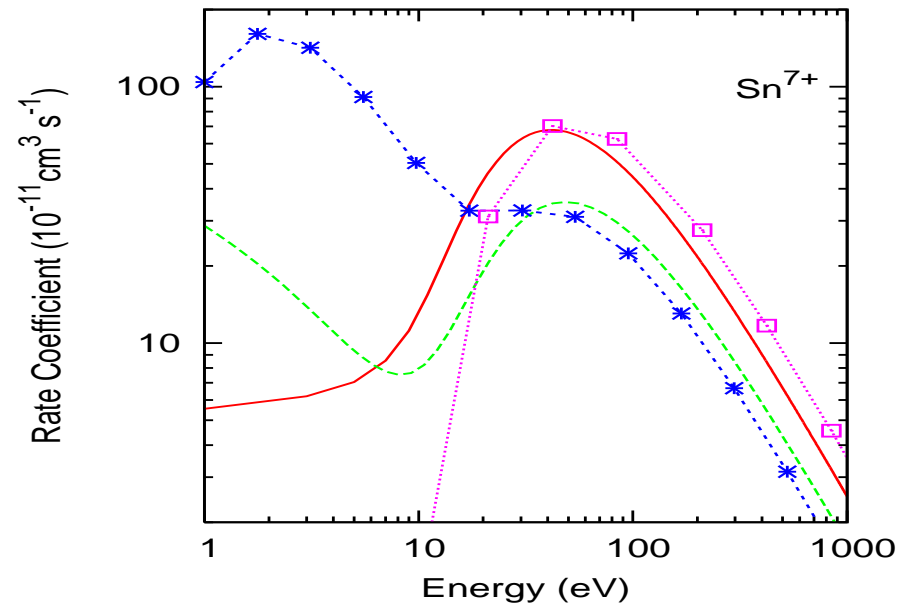
Sn⁸⁺: Total DR



Total dielectronic recombination rate coefficients for Sn⁸⁺. Solid (red) curve: configuration-average; long-dashed (green) curve: AUTOSTRUCTURE averaged over the initial ground level; short-dashed (blue) curve: Burgess-Bethe General Program averaged over the initial ground level; dotted (purple) curve; Burgess General Formula. All this work.

- CA results are about 55% larger and the BBGP 40% smaller than the AUTOSTRUCTURE results at the high temperature peak.

Sn⁷⁺: Total DR



Total dielectronic recombination rate coefficients for Sn⁷⁺. Solid (red) curve: configuration-average; long-dashed (green) curve: AUTOSTRUCTURE averaged over the initial ground level; short-dashed (blue) curve: Burgess–Bethe General Program averaged over the initial ground level; dotted (purple) curve; Burgess General Formula. All this work.

- CA results are about 100% larger and the BBGP 30% smaller than the AUTOSTRUCTURE results at the high temperature peak.

Summary

- Dipole $\Delta n = 0$ promotions dominate. This behaviour is in contrast to that found for W^{35+} (which is isoelectronic with Sn^{11+}) where both non-dipole and $\Delta n = 1$ promotions made notable contributions.
- Configuration-mixing between $4p^6 4d^{(q-1)} 4f$ and $4p^5 4d^{(q+1)}$ has a small effect on the total dielectronic recombination rate coefficient. This is despite the significant effect it has on individual radiative rates for example. Unitarity dominates.
- The BBGP results are systematically lower than those obtained from AUTOSTRUCTURE. In some cases they are significantly lower (by a factor of two).
- The CA results are systematically and significantly higher (by up to 80%) than the configuration mixed Breit–Pauli results obtained from AUTOSTRUCTURE. Their improvement over results obtained from the Burgess GF is marginal at best. This is in contrast to that found previously for W^{35+} and appears to be due to the lower residual charge here.
- The AUTOSTRUCTURE results differ significantly (by up to 70%) between averaging over just the (weight of the) ground level and all levels of the ground configuration.

Future Work

- Similar calculations for Tungsten d-shell — need to re-investigate use of AUTOSTRUCTURE vs CA: previous good agreement for W^{35+} was obtained by averaging over levels of the ground configuration.
- Begin to explore the f-shell: W^{13+} – W^{27+} — likely that BBGP/CA will play a greater role.

References

Badnell N R, Foster A, Griffin D C, Kilbane D, O Mullane M and Summers H P 2010 *J. Phys. B: At. Mol. Opt. Phys.* To be submitted (Sn^{5+} – Sn^{13+})

Badnell N R, O Mullane M G, Summers H P, Altun Z, Bautista M A, Colgan J, Gorczyca T W, Mitnik D M, Pindzola M S and Zatsarinny O 2003 *Astron. Astrophys.* **406** 1151–65 (BBGP)

Ballance C P, Loch S D, Pindzola M S and Griffin D C 2010 *J. Phys. B: At. Mol. Opt. Phys.* **43** 205201(9) (W^{35+})

Fu Y-B, Dong C-Z, Su M-G and O'Sullivan G 2007 *Chin. Phys. Lett.* **25** 927–9 (FAC Sn^{10+})

Griffin D C, Pindzola M S and Bottcher C 1985 *Phys. Rev.* **A31** 568–75 (CA)